Intrinsic Coordination Properties of Iron: Gas-Phase Ligation of Ground-State Fe^+ with Alkanes, Alkenes, and Alkynes and Intramolecular Interligand Interactions Mediated by Fe^+

Vladimir Baranov, Hansjürgen Becker,† and Diethard K. Bohme*

Department of Chemistry and Centre for Research in Earth and Space Science, York University, North York, Ontario, Canada M3J 1P3

Received: January 13, 1997; In Final Form: May 6, 1997[⊗]

The kinetics and mode of coordination of the electronic ground state $Fe^+(^6D)$ have been investigated in the gas phase with the organic molecules methane, ethane, propane, butane, ethylene, allene, propene, 1,3-butadiene, isobutene, acetylene, propyne, and diacetylene. Reaction rate coefficients and product distributions for sequential ligation were measured with the selected-ion flow tube (SIFT) technique operating at 294 ± 3 K and a helium buffer-gas pressure of 0.35 ± 0.01 Torr. Also, bond connectivities in the ligated species were probed with multicollision-induced dissociation (CID) experiments. Rates of ligation with a single ligand were found to increase with an increasing number of degrees of freedom, or size, of the ligand and to follow the reactivity order alkynes > alkenes > alkanes. Ligation with at least two, at least three, and at least five molecules was observed with alkanes, alkenes and alkynes, respectively. Possible modes of bonding in the multiply-ligated Fe^+ cations are briefly described. The CID results provide evidence for the occurrence of intramolecular interactions *between ligands* mediated by Fe^+, resulting in C−C bond formation in the ligated ions $Fe(1,3\text{-}C_4H_6)_4^+$, $Fe(C_2H_2)_3^+$ and $Fe(C_2H_2)_5^+$, $Fe(CH_3C_2H)_2^+$ and $Fe(CH_3C_2H)_4^+$, and $Fe(C_4H_2)_2^+$ and $Fe(C_4H_2)_4^+$. The postulated interligand interactions are attributed to cyclization or oligomerization reactions leading to the formation of benzene, dimethylcyclobutadiene, and diethynylcyclobutadiene in $Fe(C_2H_2)_3^+$, $Fe(CH_3C_2H)_2^+$, and $Fe(C_4H_2)_2^+$, respectively, and the formation of a dimer of 1,3-butadiene in $Fe(1,3\text{-}C_4H_6)_4^+$.

Introduction

The organic chemistry of transition-metal ions in the gas phase has been actively investigated in the past, both experimentally and theoretically.[1] Previous studies involving Fe^+ and small hydrocarbons have focused on the thermodynamic, structural, and electronic properties of the bonding of Fe^+ to single ligand molecules with a view to elucidating mechanistic and energetic aspects of C−C and C−H bond activation and insertion important in catalysis and synthetic organometallic chemistry. The small hydrocarbons which have received attention include methane,[2] ethane,[3] propane,[4] butane,[4b] ethylene,[5] acetylene,[6] propene,[5a,7] allene,[8] propyne,[8] and butenes.[5a] Here we focus on the experimental measurement of the gas-phase, room-temperature *rates* of both *single* and *multiple* ligation of Fe^+ with these and other related hydrocarbons under multicollision conditions and on the experimental determination of bond connectivities in the resulting singly- and multiply-ligated species. Such gas-phase measurements provide a useful benchmark for solution behavior and insight into *intrinsic* aspects of ligation not accessible in solution.

Experimental investigations of the room-temperature kinetics of Fe^+ ligation have not been very common in the past, although these too can provide insights into thermodynamic aspects of Fe^+−ligand bonding. Furthermore, the earlier investigations have been restricted to single-ligation kinetics. Fast-flow reactor,[9] crossed-beam,[4b] "chromatographic",[10] and FT-ICR[11] experiments have shown that methane, ethane, and propane will ligate Fe^+ at room temperature in He bath gas by collision-stabilized attachment with measurable rates but that ligation competes with activation/insertion leading to dissociative addition with propane and butane, particularly at higher collision energies and lower pressures. Slow ligation of Fe^+ with ethylene, propene, and isobutene has been observed at low pressures.[5a] Similar measurements with the remaining alkenes and the alkynes investigated in this study appear not to have been reported previously. A single potential-well model has been presented for reactions of Fe^+ with small alkanes which elucidates the critical role of the lifetime of the intermediate adduct ion in determining the rates of ligation observed in a multicollision environment.[9b] The model predicts that the rate of ligation depends on the size of hydrocarbon ligand and on the thermodynamic stability of the ligated FeL^+ ion (where L is the ligand).

Multiple ligation of Fe^+ with hydrocarbons in the gas phase may be achieved in at least two ways: by sequential termolecular ligation reactions of type 1 beginning with unligated Fe^+ or by sequential bimolecular "switching" reactions of type 2 beginning with Fe^+ already ligated, but with a different ligand.

$$FeL_n^+ + L + He \rightarrow FeL_{n+1}^+ + He \quad (1)$$

$$FeL'_nL''_m + L'' \rightarrow FeL'_{n-1}L''_{m+1} + L' \quad (2)$$

Sequential ligation of type 1 was first observed in fast-flow reactor experiments which provided evidence for the multiple ligation of Fe^+ with methane, ethane, and propane in helium bath gas at 0.75 Torr, although rate coefficients were not determined. Not much is known quantitatively about the sequential kinetics of either reactions 1 or reactions 2, but their occurrence has been exploited in the past in the generation of multiply-ligated FeL_n^+ ions for studies of their energetics and structures. For example, $Fe(CH_4)_n^+$ ions with $n = 1-4$ have been generated from reactions of type 1 in collision-induced

† Fakultät Umweltwissenschaften und Verfahrenstechnik, Brandenburgische Technische Universität Cottbus, Karl-Marx-Strasse 17, D-03044 Cottbus, Germany.

* Corresponding author.

⊗ Abstract published in *Advance ACS Abstracts,* June 15, 1997.

S1089-5639(97)00186-2 CCC: $14.00

dissociation studies of the ligand binding energies in these ions,[2a] and $Fe(CO)_n^+$ ions have been transformed into $Fe(C_2H_4)^+$ and $Fe(C_2H_2)_n^+$ ($n = 1-4$) ions according to reaction 2 in a chemical ionization source in recent NRMS experiments directed toward the elucidation of the structures of these ions.[5c,10] The latter study[10] also provided the first evidence for the Fe^+−mediated trimerization of C_2H_2 to benzene. This interesting result suggests a potential role of Fe^+ in promoting C−C bond formation and in the mediation of ligand/ligand reactions generally.

In this study we have surveyed the interactions of Fe^+ with selected alkanes, alkenes, and alkynes in a multicollision environment. Two experimental approaches were used. Sequential addition of ligands to Fe^+ was explored through measurements of rate coefficients for reactions of type 1 in helium bath gas at 0.35 Torr using the selected-ion flow tube (SIFT) technique. This is a moderately high-pressure technique which provides the multiple collisions required for the third-body stabilization of the ligated ions FeL_n^+ ions. The results of these measurements provide insight into the dependence of rates of ligation on the number and size of ligands and on the thermodynamic stability of the ligated ion. Also, they provide intrinsic reactivities and coordination numbers which are useful in understanding analogous coordination reactions in solution.

Also, we have conducted multicollision-induced dissociation (CID) experiments to explore bond connectivities in the ligated ions directly after their formation and collisional stabilization. These experiments have revealed the occurrence of several novel intramolecular interligand reactions and speak to the possible role of Fe^+ as a catalyst for cyclization and oligomerization of unsaturated hydrocarbons.

Experimental Section

The results reported here were obtained using a selected-ion flow tube (SIFT) apparatus which has been described previously.[13,14] All measurements were performed at 294 ± 3 K and at helium buffer gas pressure of 0.35 ± 0.01 Torr. The reactant Fe^+ ions were produced in a low-pressure ionization source either from $Fe(CO)_5$ by 35−50 eV electron bombardment or from ferrocene vapor at 60−70 eV, mass selected, injected into the flow tube, and allowed to thermalize by collisions (ca. 4×10^5) with He atoms before entering the reaction region. Both $Fe(CO)_5$ and ferrocene were introduced into the ion source in a large excess of helium (at a partial pressure of less than 5%). The ion signal showed a maximum with increasing pressure which is suggestive of ion/He collisions within the source and the occurrence of dissociative electron-transfer reactions of He^+ with the parent gas. Normally the ion signal was tuned at the maximum. As we have reported elsewhere, we could not find any evidence for the presence of excited states of Fe^+ in our reacting Fe^+ population.[15]

Reactant neutrals were introduced into the reaction region either as a pure gas or as a dilute (0.2−5%) mixture in helium. All the reagents except diacetylene were obtained commercially and were of high purity (generally >99%). Diacetylene was synthesized by reacting 1,4-dichloro-2-butyne with aqueous KOH in DMSO solution.[16]

The rate coefficients for primary reactions reported here are estimated to have an uncertainty of ±30%. Higher-order rate coefficients were obtained by fitting the experimental data to the solutions of the system of differential equations for successive reactions. The accuracy for this fitting procedure depends on several parameters and is reported separately for every calculated high-order rate coefficient.

The multicollision-induced dissociation (CID) of sampled ions was investigated by raising the potential of the sampling nose cone while taking care not to introduce mass discrimination in the detection system. This technique has been developed in our laboratory recently and is described in detail elsewhere.[17] The technique is most useful for the exploration of bond connectivities in that ion fragmentation can be induced in a controlled stepwise fashion. However, since the concomitant energy redisposition has not yet been successfully modeled, the observed thresholds for dissociation do not yield precise thermodynamic information. Bond connectivity studies become problematic when the ion of interest is one of several ions being sampled, viz. cannot be established as the predominant ion, or when it has too low an intensity.

Results and Discussion

Table 1 summarizes the products and rate coefficients measured for the primary and higher-order reactions of Fe^+ with selected alkanes, alkenes, and alkynes at 294 ± 3 K in helium buffer gas at a total gas pressure of 0.35 ± 0.01 Torr.

A. Reactions with Alkanes: CH_4, C_2H_6, C_3H_8, and C_4H_{10}. The effective bimolecular rate coefficients measured for the association reactions of Fe^+ with alkanes under our SIFT conditions span a large range from $<5 \times 10^{-14}$ cm^3 molecule^{-1} s^{-1} for the reaction with methane to 1.0×10^{-9} cm^3 molecule^{-1} s^{-1} for the reaction with *n*-butane. Representative data for the observed chemistry and CID are shown in Figures 1−3. With the exception of the reaction with *n*-butane, only adduct formation was observed under our operating conditions. The failure to observe bimolecular products with methane and ethane is not surprising since these should be endothermic. However, bimolecular channels do become exothermic with propane and higher saturated hydrocarbons. Indeed, reactions 3a and 3b

$$Fe^+ + C_3H_8 \rightarrow FeC_3H_6^+ + H_2 \quad (3a)$$

$$\rightarrow FeC_2H_4^+ + CH_4 \quad (3b)$$

which are exothermic by 11 ± 5 and 19 ± 5 kcal mol^{-1}, respectively,[4b] have been observed as minor channels with both the flow reactor in He at 0.75 Torr[9b] and the chromatographic technique in He at 1.75 Torr.[10] The fast-flow reactor measurements yielded branching ratios of 2.0 ± 0.4 and 4.3 ± 0.3%, respectively, while the chromatographic technique led to branching ratios of 1.4 and 3%, respectively. However, our experiments indicated an upper limit of 1% for both of these channels and that collisional stabilization completely dominates. The reason for this discrepancy is not clear. One possible explanation is that the previous measurements, in which Fe^+ ions were produced differently, included some contribution from the excited ^{4}F state of Fe^+: both channels 3a and 3b are major channels in reactions with this state.[4b,10] It is interesting to note that, at the very low pressures of 3×10^{-7} Torr at which collisional stabilization is improbable, FT-ICR experiments have shown that Fe^+ reacts with propane exclusively to yield the bimolecular channels 3a and 3b in a ratio of 24/76.[11]

Bimolecular channels definitely become competitive under our experimental operating conditions in the reaction of Fe^+ with *n*-butane. The data in Figure 3 shows the occurrence of the reaction channels 4a−4d. Analysis of this data provides a

$$Fe^+ + n\text{-}C_4H_{10} \rightarrow FeC_4H_{10}^+ \quad (4a)$$

$$\rightarrow FeC_2H_4^+ + C_2H_6 \quad (4b)$$

$$\rightarrow FeC_3H_6^+ + CH_4 \quad (4c)$$

$$\rightarrow FeC_4H_8^+ + H_2 \quad (4d)$$

TABLE 1: Measured Products and Rate Coefficients for Reactions of Ground-State Fe^+ Cations with Selected Alkanes, Alkenes, and Alkynes at 294 ± 3 K in Helium Buffer Gas at a Total Pressure of 0.35 ± 0.01 Torr; Reaction[a] and Collision[b] Rate Coefficients Are Given in Units of cm^3 $molecules^{-1}$ s^{-1}

reactant molecule	reactant/product ions[c]	k_{exp}	k_c	k_{exp}/k_c
CH_4	$Fe^+/Fe(CH_4)^+$	$<5 \times 10^{-14}$	1.1×10^{-9}	$<5 \times 10^{-5}$
	$Fe(CH_4)^+/$	*d*		
C_2H_6	$Fe^+/Fe(C_2H_6)^+$	1.4×10^{-11}	1.1×10^{-9}	0.013
	$Fe(C_2H_6)^+/Fe(C_2H_6)_2^+$	3.7×10^{-10}		
	$Fe(C_2H_6)_2^+$	$<5 \times 10^{-14}$		
C_3H_8	$Fe^+/Fe(C_3H_8)^+$	3.9×10^{-10}	1.2×10^{-9}	0.33
	$Fe(C_3H_8)^+/Fe(C_3H_8)_2^+$	7.3×10^{-10}		
	$Fe(C_3H_8)_2^+$	$<5 \times 10^{-14}$		
C_4H_{10}	$Fe^+/Fe(C_4H_{10})^+$ 0.40	1.0×10^{-9}	1.2×10^{-9}	0.83
	$Fe^+/Fe(C_2H_4^+)$ 0.38			
	$Fe^+/Fe(C_3H_6^+)$ 0.13			
	$Fe^+/Fe(C_4H_8^+)$ 0.09			
	$Fe(C_4H_{10})^+/Fe(C_4H_{10})_2^+$	7.8×10^{-10}		
	$Fe(C_4H_{10})_2^+$	$<1 \times 10^{-13}$		
C_2H_4	$Fe^+/Fe(C_2H_4)^+$	6.1×10^{-11}	1.1×10^{-9}	0.055
	$Fe(C_2H_4)^+/Fe(C_2H_4)_2^+$	6.3×10^{-10}		
	$Fe(C_2H_4)_2^+/Fe(C_2H_4)_3^+$	8.7×10^{-11}		
	$Fe(C_2H_4)_3^+/Fe(C_2H_4)_4^+$	$(3.0 \pm 1.5) \times 10^{-13}$		
	$Fe(C_2H_4)_4^+/$	*d*		
C_3H_4 (allene)	$Fe^+/Fe(C_3H_4)^+$	2.1×10^{-10}	1.2×10^{-9}	0.18
	$Fe(C_3H_4)^+/Fe(C_3H_4)_2^+$	6.0×10^{-10}		
	$Fe(C_3H_4)_2^+/Fe(C_3H_4)_3^+$	2.2×10^{-10}		
	$Fe(C_3H_4)_3^+$	$<1 \times 10^{-13}$		
C_3H_6 (propene)	$Fe^+/Fe(C_3H_6)^+$	3.9×10^{-10}	1.3×10^{-9}	0.30
	$Fe(C_3H_6)^+/Fe(C_3H_6)_2^+$	3.9×10^{-10}		
	$Fe(C_3H_6)_2^+/Fe(C_3H_6)_3^+$	3.3×10^{-10}		
	$Fe(C_3H_6)_3^+$	$<1 \times 10^{-13}$		
C_4H_6 (1,3-butadiene)	$Fe^+/Fe(C_3H_6)^+$	8.4×10^{-10}	1.3×10^{-9}	0.65
	$Fe(C_3H_6)^+/Fe(C_3H_6)_2^+$	8.5×10^{-10}		
	$Fe(C_3H_6)_2^+/Fe(C_3H_6)_3^+$	3.3×10^{-12}		
	$Fe(C_3H_6)_3^+/Fe(C_3H_6)_4^+$	*e*		
	$Fe(C_3H_6)_4^+/$	*d*		
i-C_4H_8 (isobutene)	$Fe^+/Fe(C_4H_8)^+$	8.9×10^{-10}	1.4×10^{-9}	0.64
	$Fe(C_4H_8)^+/Fe(C_4H_8)_2^+$	1.1×10^{-9}		
	$Fe(C_4H_8)_2^+/Fe(C_4H_8)_3^+$	5.3×10^{-12}		
	$Fe(C_4H_8)_3^+$	$<1 \times 10^{-13}$		
C_2H_2	$Fe^+/Fe(C_2H_2)^+$	1.6×10^{-11}	1.1×10^{-9}	0.015
	$Fe(C_2H_2)^+/Fe(C_2H_2)_2^+$	7.7×10^{-10}		
	$Fe(C_2H_2)_2^+/Fe(C_2H_2)_3^+$	7.6×10^{-10}		
	$Fe(C_2H_2)_3^+/Fe(C_2H_2)_4^+$	$(2 \pm 1) \times 10^{-12}$		
	$Fe(C_2H_2)_4^+/Fe(C_2H_2)_5^+$	$(5 \pm 2) \times 10^{-12}$		
	$Fe(C_2H_2)_5^+/Fe(C_2H_2)_6^+$	*e*		
	$Fe(C_2H_2)_6^+/$	*d*		
C_3H_4 (propyne)	$Fe^+/Fe(C_3H_4)^+$	7.0×10^{-10}	1.5×10^{-9}	0.47
	$Fe(C_3H_4)^+/Fe(C_3H_4)_2^+$	7.5×10^{-10}		
	$Fe(C_3H_4)_2^+/Fe(C_3H_4)_3^+$	6.0×10^{-10}		
	$Fe(C_3H_4)_3^+/Fe(C_3H_4)_4^+$	$(6 \pm 3) \times 10^{-12}$		
	$Fe(C_3H_4)_4^+/Fe(C_3H_4)_5^+$	$(7 \pm 4) \times 10^{-12}$		
	$Fe(C_3H_4)_5^+/Fe(C_3H_4)_6^+$	*e*		
	$Fe(C_3H_4)_6^+/$	*d*		
C_4H_2 (diacetylene)	$Fe^+/Fe(C_4H_2)^+$	3.5×10^{-10}	1.2×10^{-9}	0.29
	$Fe(C_4H_2)^+/Fe(C_4H_2)_2^+$	1.0×10^{-9}		
	$Fe(C_4H_2)_2^+/Fe(C_4H_2)_3^+$	3.0×10^{-10}		
	$Fe(C_4H_2)_3^+/Fe(C_4H_2)_4^+$	$(9 \pm 5) \times 10^{-12}$		
	$Fe(C_4H_2)_4^+/Fe(C_4H_2)_5^+$	$(1.0 \pm 0.5) \times 10^{-11}$		
	$Fe(C_4H_2)_5^+/Fe(C_4H_2)_6^+$	*e*		
	$Fe(C_4H_2)_6^+/$	*d*		

[a] The uncertainty in the reaction rate coefficient is less than 30%, unless indicated otherwise. [b] The collision rate coefficient is calculated using ADO theory.[16] [c] The branching ratios are indicated for the reaction with *n*-butane. Products which were observed not to be formed are not indicated. [d] Not observed. [e] Observed.

branching ratio for (4a)/(4b)/(4c)/(4d) of 0.40/0.38/0.13/0.09. The bimolecular channels outweigh the association channel by 3 to 2. The branching ratio of the bimolecular channels (4b)/(4c)/(4c) of 0.67/0.22/0.15 is consistent with the trend reported recently for the production of these channels in crossed-beam experiments at kinetic energies of 1.1 and 0.25 eV.[4b] The reported branching ratios for the reaction of ground-state Fe^+-(^{6}D) at these kinetic energies were 0.39/0.43/0.18 and 0.58/0.32/0.10, respectively. We did not completely unravel the secondary chemistry evident in Figure 3, although it is clear that the $FeC_4H_8^+$ product ion is less reactive, $k = (5.5 \pm 1.7) \times 10^{-11}$ cm^3 $molecule^{-1}$ s^{-1}, than the other three product ions of reaction 4 which all react further with an identical rate coefficient, within experimental uncertainty, of $(7.8 \pm 2.3) \times 10^{-10}$ cm^3 $molecule^{-1}$ s^{-1}. The product spectrum for the secondary reactions shown in Figure 3 is consistent with *n*-butane adduct formation involving these three product ions accompanied by varying degrees of elimination of C_2H_6, CH_4, and H_2.

The reactions of Fe^+ with methane, ethane, and propane have been investigated previously at thermal energies with a fast flow

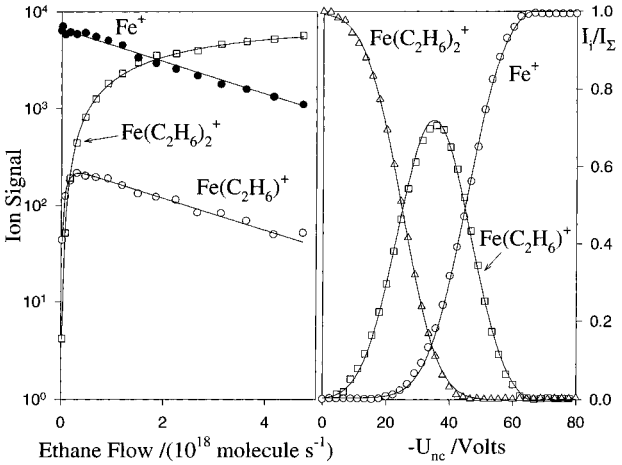

Figure 1. (left) Experimental data for the reaction of Fe^+ with ethane. The solid lines represent a fit of the experimental data with the solutions of differential equations appropriate for the observed sequential reactions. (right) Multicollisional CID of $Fe(C_2H_6)_2^+$ in helium at 0.35 Torr in the laboratory energy frame. The ethane flow is equal to 7.0×10^{18} molecule s^{-1}.

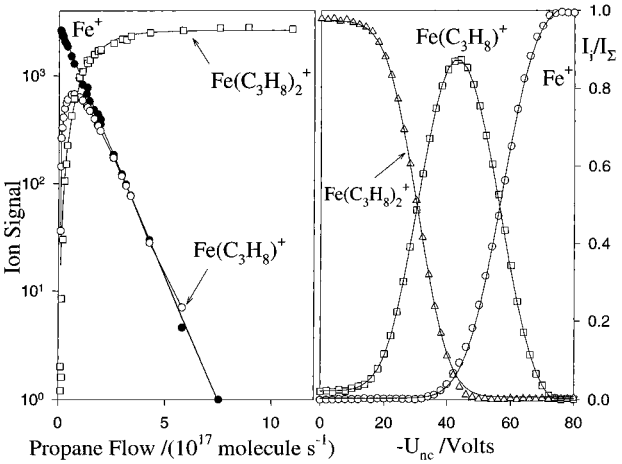

Figure 2. (left) Experimental data for the reaction of Fe^+ with propane. The solid lines represent a fit of the experimental data with the solutions of differential equations appropriate for the observed sequential reactions. (right) Multicollisional CID of $Fe(C_3H_8)_2^+$ in helium at 0.35 Torr in the laboratory energy frame. The propane flow is equal to 6.0×10^{17} molecule s^{-1}.

reactor at the higher helium pressure of 0.75 Torr. Rate coefficients of $(1.1 \pm 0.3) \times 10^{-12}$, $(5.9 \pm 1.8) \times 10^{-11}$, and $(6.2 \pm 1.9) \times 10^{-10}$ cm^3 $molecule^{-1}$ s^{-1} have been reported for these conditions.[9b] A rate coefficient of $(5.0 \pm 1.5) \times 10^{-10}$ cm^3 $molecule^{-1}$ s^{-1} has been reported for the addition of propane at the still higher helium pressure of 1.75 Torr at 300 K.[10] These values are all systematically higher than those measured in our study and clearly point toward a dependence of the reaction rate on pressure as is expected if the ligation proceeds by termolecular association with collisional stabilization. An appropriate kinetic model for third-body collisional stabilization in reactions of Fe^+ with small alkanes has been discussed in detail by Weisshaar et al.[9b] The model predicts that the effective bimolecular rate coefficient should increase with increasing pressure and saturate at a value equal to the Langevin collision rate coefficient. The trend in k_{exp} with pressure is clearly evident in Figure 4 in which the size of the alkane is expressed in terms of its number of degrees of freedom. The trend in the effective bimolecular rate coefficient with the size of the alkane will be discussed later.

What can be said about the number of alkane ligands that add sequentially to Fe^+? Only the first adduct was observed

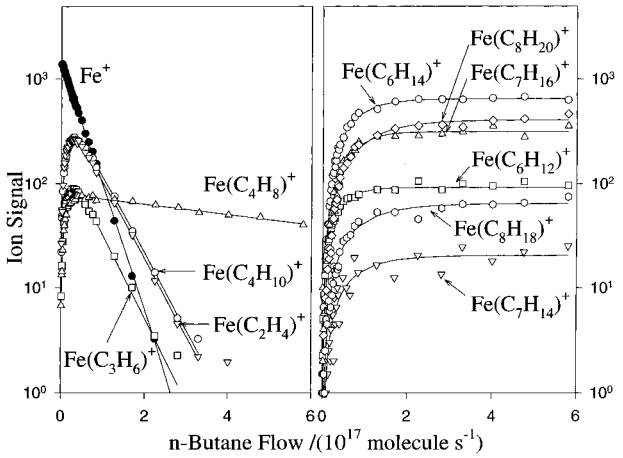

Figure 3. (left) Experimental data for the primary reactions of Fe^+ with butane. (right) Experimental data for the secondary reactions of Fe^+ with butane. The solid lines represent a fit of the experimental data with the solutions of differential equations appropriate for the observed sequential reactions.

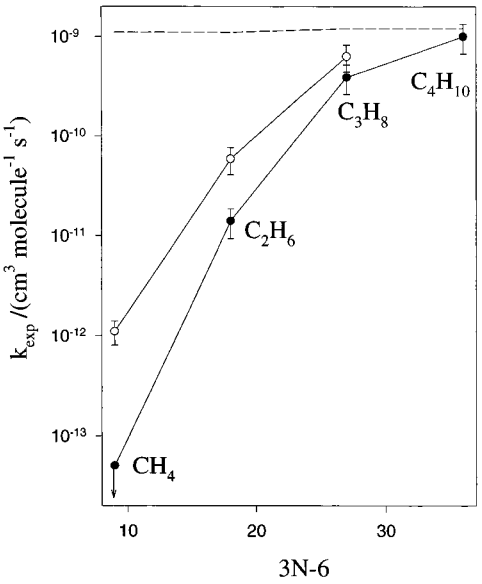

Figure 4. Variation in the effective bimolecular rate coefficient for the reaction of Fe^+ with alkanes with the size of the alkane expressed in terms of its number of degrees of freedom (*N* is the number of atoms). Open circles represent the data of Weisshaar et al.[9b] taken with a fast-flow reactor at a helium pressure of 0.75 Torr. The solid circles represent the SIFT data obtained in this study at a helium pressure of 0.35 ± 0.01 Torr. The dashed curve represents the variation of the bimolecular Langevin collision rate constant.

when Fe^+ reacted with methane under our SIFT conditions, and it was formed with an immeasurably small rate coefficient. In previous measurements with a fast-flow reactor at the higher helium pressure of 0.75 Torr, up to three additions were observed, although rate coefficients were not reported for additions of more than one methane molecule.[9b] $Fe(CH_4)_n^+$ ions with *n* as large as 4 have been generated in a dc discharge/flow tube source.[2a]

Our SIFT experiments have shown that two molecules of ethane and propane rapidly add sequentially to Fe^+ and in both cases the second molecule adds with a higher rate: about 25 times higher in the case of ethane and 2 times higher in the case of propane. The rate of ligation drops precipitously for the formation of the third adduct, by a factor of at least 7×10^3 in both cases, and the third adduct was not observed. These results agree with those obtained using the fast-flow reactor which indicated that two, but not three, molecules of ethane

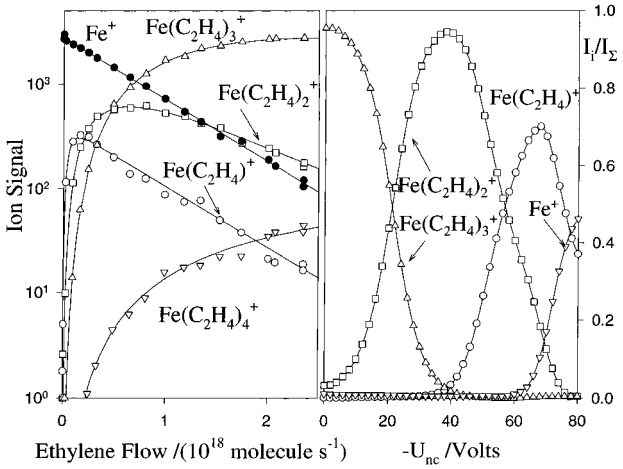

Figure 5. (left) Experimental data for the reaction of Fe^+ with ethylene. The solid lines represent a fit of the experimental data with the solutions of differential equations appropriate for the observed sequential reactions. (right) Multicollisional CID of $Fe(C_2H_4)_3^+$ in helium at 0.35 Torr in the laboratory energy frame. The ethylene flow is equal to 3.9×10^{18} molecule s^{-1}.

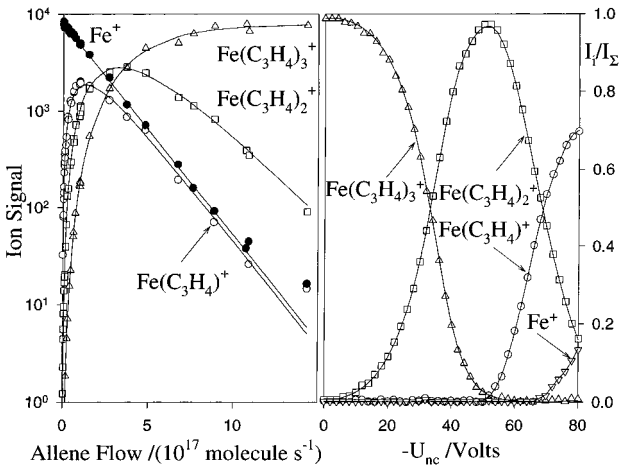

Figure 6. (left) Experimental data for the reaction of Fe^+ with allene. The solid lines represent a fit of the experimental data with the solutions of differential equations appropriate for the observed sequential reactions. (right) Multicollisional CID of $Fe(C_3H_4)_3^+$ in helium at 0.35 Torr in the laboratory energy frame. The allene flow is equal to 1.6×10^{18} molecule s^{-1}.

and two molecules of propane added sequentially at the higher He pressure of 0.75 Torr; again however, rate coefficients for the addition of more than one molecule were not reported for these latter experiments.[9b] Our results with butane also indicate rapid sequential addition of only two molecules. The third addition was immeasurably slow, and no third adduct was observed.

The CID profiles in Figures 1 and 2 show clearly that ligated ethane molecules and ligated propane molecules do not react with each other in the presence of Fe^+. Collisional activation of the ligated ions removes these molecules sequentially one at a time in a manner reverse to the sequential addition.

We take our kinetic and CID results to indicate that Fe^+ has a coordination number of 2 with the alkane molecules ethane, propane, and butane.

B. Reactions with Alkenes: C_2H_4, C_3H_6, $H_2C{=}C{=}CH_2$, 1,3-C_4H_6, and *i*-C_4H_8. To the extent that standard enthalpies of formation are available, thermodynamics predicts that bimolecular reactions, including electron transfer, are energetically unfavorable with ethylene, propene, allene, 1,3-butadiene, and isobutene. Only sequentail ligation reactions were observed

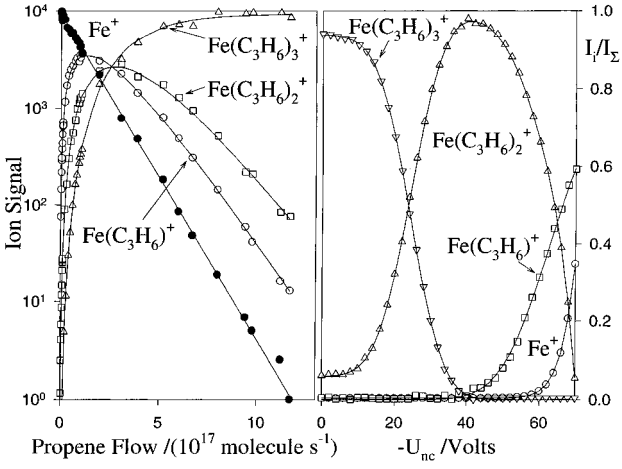

Figure 7. (left) Experimental data for the reaction of Fe^+ with propene. The solid lines represent a fit of the experimental data with the solutions of differential equations appropriate for the observed sequential reactions. (right) Multicollisional CID of $Fe(C_3H_6)_3^+$ in helium at 0.35 Torr in the laboratory energy frame. The propene flow is equal to 6.7×10^{17} molecule s^{-1}.

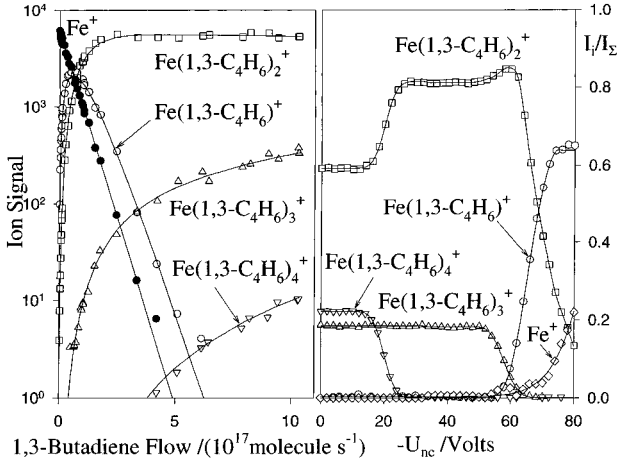

Figure 8. (left) Experimental data for the reaction of Fe^+ with 1,3-butadiene. The solid lines represent a fit of the experimental data with the solutions of differential equations appropriate for the observed sequential reactions. (right) Multicollisional CID of $Fe(1,3\text{-}C_4H_6)_n^+$ with $n = 2$, 3, and 4 in helium at 0.35 Torr in the laboratory energy frame. The flow of 1,3-butadiene is equal to 5.3×10^{18} molecule s^{-1}.

under our operating conditions with these five alkenes. Representative data are shown in Figures 5−9. Again, the effective bimolecular rate coefficient for the first addition increases substantially with increasing size of the alkene, viz. from 6.1×10^{-11} cm^3 $molecule^{-1}$ s^{-1} for the reaction with ethylene to 8.9×10^{-10} cm^3 $molecule^{-1}$ s^{-1} for the reaction with isobutene.

The number of alkene molecules observed to add sequentially to Fe^+ was at least three, but four molecules were seen to add with ethylene and 1,3-butadiene. A drop in rate by at least a factor of 10^2 was observed after the addition of three molecules except with the larger alkenes, 1,3-butadiene and isobutene, for which such a drop occurred already after the addition of two molecules. The CID experiments indicated sequential loss of individual molecules from all triply-ligated species. However, Figure 8 clearly shows that the quadruply-ligated species Fe-(1,3-C_4H_6)$_4^+$ dissociates in one step exclusively with the loss of the equivalent of two molecules of 1,3-butadiene according to reaction 5.

$$Fe(1,3\text{-}C_4H_6)_4^+ + He \rightarrow Fe(1,3\text{-}C_4H_6)_2^+ + [(1,3\text{-}C_4H_6)_2] + He \quad (5)$$

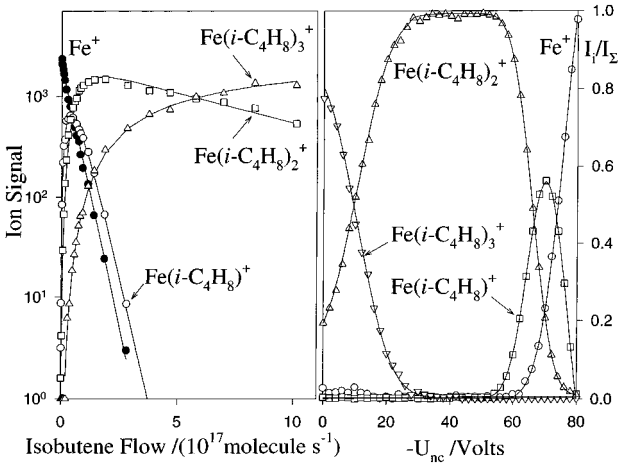

Figure 9. (left) Experimental data for the reaction of Fe^+ with isobutene. The solid lines represent a fit of the experimental data with the solutions of differential equations appropriate for the observed sequential reactions. (right) Multicollisional CID of $Fe(i\text{-}C_4H_8)_3^+$ in helium at 0.35 Torr in the laboratory energy frame. The isobutene flow is equal to 9.1×10^{17} molecule s^{-1}.

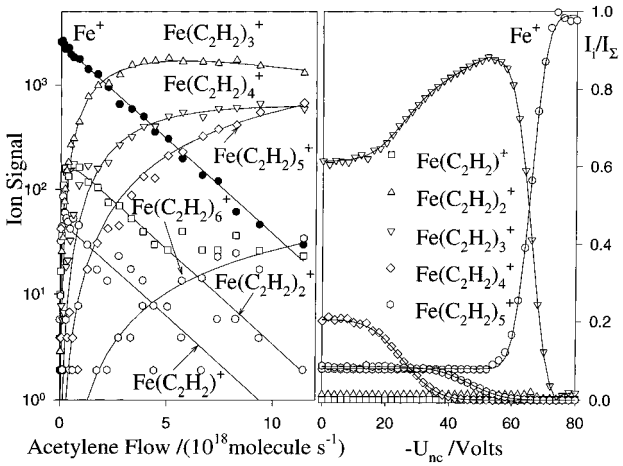

Figure 10. (left) Experimental data for the reaction of Fe^+ with acetylene. The solid lines represent a fit of the experimental data with the solutions of differential equations appropriate for the observed sequential reactions. (right) Multicollisional CID of $Fe(C_2H_2)_n^+$ with $n = 3$, 4, and 5 in helium at 0.35 Torr in the laboratory energy frame. The flow of acetylene is equal to 6.0×10^{18} molecule s^{-1}.

C. Reactions with Alkynes: C_2H_2, CH_3C_2H, and C_4H_2.

Only sequential ligation was observed in the reactions of Fe^+ with acetylene, propyne, and diacetylene. Representative data are shown in Figures 10−12. The measured effective bimolecular rate coefficient for the first addition increases from 1.6×10^{-11} cm^3 $molecule^{-1}$ s^{-1} for the addition of C_2H_2 to 3.5×10^{-10} and 7.5×10^{-10} cm^3 $molecule^{-1}$ s^{-1} for the first addition of C_4H_2 and CH_3C_2H, respectively.

At least six alkyne molecules were observed to add sequentially to Fe^+, but as was the case with the alkenes, a sharp drop in rate (by at least a factor of 30 in this case) was observed after the addition of three molecules. But the rate coefficient did not become immeasurably small. Two further additions were observed with measurable rates, and the addition of another acetylene to form $Fe(C_2H_2)_6^+$ was also recorded.

The CID experiments indicated a variety of different types of behavior for the dissociation of alkyne-ligated Fe^+ species. Loss of individual molecules was observed to be less common than for the alkane- and alkene-ligated species. Figure 10 shows that the triply-ligated species $Fe(C_2H_2)_3^+$ dissociates in one step exclusively with the loss of the equivalent of three molecules

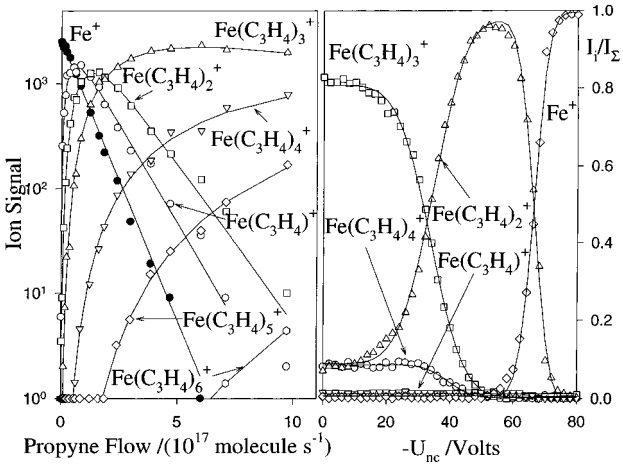

Figure 11. (left) Experimental data for the reaction of Fe^+ with propyne. The solid lines represent a fit of the experimental data with the solutions of differential equations appropriate for the observed sequential reactions. (right) Multicollisional CID of $Fe(C_3H_4)_n^+$ with $n = 2$, 3, and 4 in helium at 0.35 Torr in the laboratory energy frame. The flow of propyne is equal to 1.7×10^{18} molecule s^{-1}.

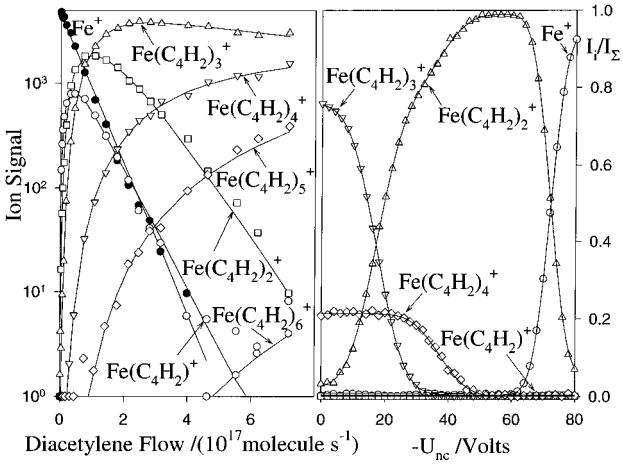

Figure 12. (left) Experimental data for the reaction of Fe^+ with diacetylene. The solid lines represent a fit of the experimental data with the solutions of differential equations appropriate for the observed sequential reactions. (right) Multicollisional CID of $Fe(C_4H_2)_n^+$ with $n = 3$ and 4 in helium at 0.35 Torr in the laboratory energy frame. The flow of diacetylene is equal to 4.8×10^{17} molecule s^{-1}.

of acetylene according to reaction 6 and that the quintuply-

$$Fe(C_2H_2)_3^+ + He \rightarrow Fe^+ + [(C_2H_2)_3] + He \qquad (6)$$

ligated $Fe(C_2H_2)_5^+$ dissociates in one step to lose the equivalent of two molecules of acteylene according to reaction 7. In

$$Fe(C_2H_2)_5^+ + He \rightarrow Fe(C_2H_2)_3^+ + [(C_2H_2)_2] + He \qquad (7)$$

comparison, Figure 11 shows that the doubly-ligated propyne species loses the equivalent of two molecules upon dissociation according to reaction 8 and that the quadruply-ligated species

$$Fe(C_3H_4)_2^+ + He \rightarrow Fe^+ + [(C_3H_4)_2] + He \qquad (8)$$

also loses the equivalent of two molecules of propyne according to reaction 9. Although the loss of just one molecule of propyne

$$Fe(C_3H_4)_4^+ + He \rightarrow Fe(C_3H_4)_2^+ + [(C_3H_4)_2] + He \qquad (9)$$

could not be completely excluded on the basis of the shape of the $Fe(C_3H_4)_3^+$ CID profile, the earlier onset for the dissociation

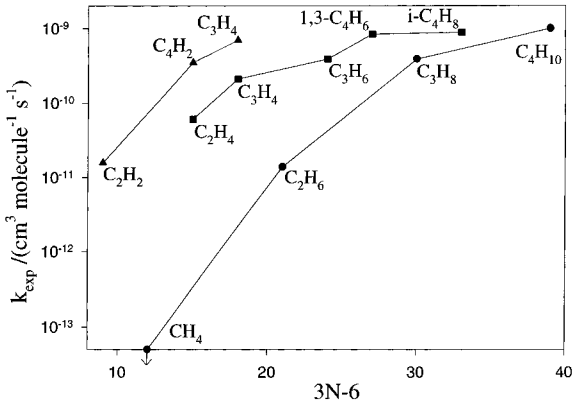

Figure 13. A semilogarithmic correlation of the effective bimolecular rate coefficient in the gas phase in helium buffer gas at 294 ± 3 K and a total pressure of 0.35 ± 0.01 Torr for the single ligation of Fe^+ with hydrocarbon molecules with the size of the hydrocarbon expressed in terms of its number of degrees of freedom (*N* is the number of atoms). Solid circles represent alkanes, solid squares represent alkenes, and solid triangles represent alkynes.

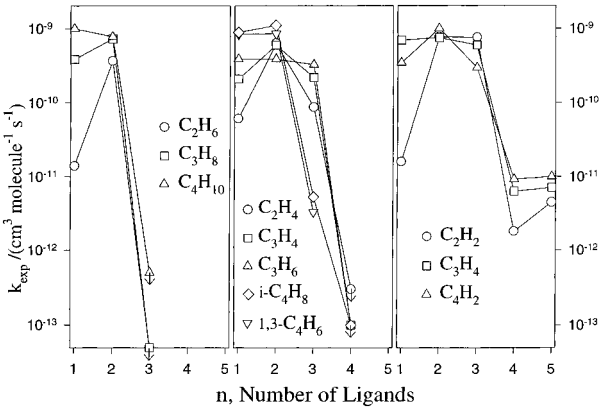

Figure 14. A semilogarithmic correlation of the effective bimolecular rate coefficient for the sequential ligation of Fe^+ with hydrocarbon molecules with the number of ligands added in the gas phase in helium buffer gas at 294 ± 3 K and a total pressure of 0.35 ± 0.01 Torr: left, alkanes; middle, alkenes; right, alkynes.

of $Fe(C_3H_4)_3^+$ implies a greater binding energy for $[(C_3H_4)_2]$ within $Fe(C_3H_4)_4^+$ which is more consistent with the occurrence of reaction 9. Figure 12 shows that the dissociation of both the doubly-ligated and quadruply-ligated diacetylene species leads to loss of two molecules according to reactions 10 and

$$Fe(C_4H_2)_2^+ + He \rightarrow Fe^+ + [(C_4H_2)_2] + He \quad (10)$$

$$Fe(C_4H_2)_4^+ + He \rightarrow Fe(C_4H_2)_2^+ + [(C_4H_2)_2] + He \quad (11)$$

11. The same order in the dissociation threshold, viz. DT-$((C_4H_2)_2Fe^+-C_4H_2)$ < DT$((C_4H_2)_2Fe^+-[(C_4H_2)_2])$, is observed in this case.

D. Variation in the Rate of Ligation with the Size of the Hydrocarbon. Figure 13 presents the dependence of the effective bimolecular rate coefficient, k_{exp}, for all of the Fe^+ addition reactions observed in this study in helium at 0.35 Torr on the number of degrees of freedom of the hydrocarbon molecule, $3N - 6$ (where *N* is the number of atoms). There is an obvious increase in reactivity with increasing size for the alkanes, alkenes, and alkynes, and the rate coefficients begin to saturate at a value corresponding to the collision rate coefficient, about 10^{-9} cm^3 molecule^{-1} s^{-1}, with the highest member of each series of hydrocarbons. Also, the relative magnitudes of the rate coefficients at a fixed number of degrees of freedom show the reactivity order alkynes > alkenes > alkanes. These trends in kinetics can be understood in terms of the single-potential well model for collisional association presented previously by Weisshaar et al. for Fe^+−alkane ligation in which variations in rate coefficients are mainly attributed to variations in the lifetime of the intermediate "hot" adduct against redissociation.[9b] This lifetime increases as the vibrational-state density of the "hot" adduct increases and is dependent directly on the vibrational degrees of freedom and the bond energy (or well depth) of the adduct. Thus, the trend in kinetics observed for alkane ligation is due both to the increasing number of degrees of freedom and the increasing bond energies of the adduct ions. It is known that the bond strength increases from 0.59 ± 0.03 eV for Fe^+-CH_4,[2a] to 0.66 ± 0.06 eV for $Fe^+-C_2H_6$[3a] and 0.78 ± 0.04 eV for $Fe^+-C_3H_8$.[4a] Differences in rate coefficients at a fixed degree of freedom must be attributed largely to differences in binding energies as, for example, the difference observed for the reactions of Fe^+ with allene and propyne. The bond energies for Fe^+−allene and Fe^+−propyne are not known, but our results predict a stronger interaction in the case of Fe^+−propyne. In comparing alkanes, alkenes, and alkynes with the same carbon content such as, for example, ethane, ethylene, and acetylene, one must consider both degrees of freedom and bond energies. Thus, while the order in bond energies is $D_0(Fe^+-C_2H_4) > D_e(Fe^+-C_2H_2) > D_0(Fe^+-C_2H_6)$ (1.50 ± 0.06[18] > 1.04[6] > 0.66 ± 0.06 eV[3a]) and the order in the number of degrees of freedom is $Fe^+-C_2H_6 > Fe^+-C_2H_4 > Fe^+-C_2H_2$, the order in the effective bimolecular rate coefficient for ligation is $k(C_2H_4) > k(C_2H_2) > k(C_2H_6)$ ($6.1 \times 10^{-11} > 1.6 \times 10^{-11} > 1.4 \times 10^{-11}$ cm^3 molecule^{-1} s^{-1}).

E. Variation in the Rate of Ligation with the Number of Ligands. The moderate helium bath-gas pressure of 0.35 Torr employed in these experiments is sufficient to allow for collisional stabilization of the hot intermediate ligated ions and so to probe the full extent of ligation, or coordination, of Fe^+ with the various hydrocarbon ligands investigated. Here the coordination number is defined in terms of the observed ligation kinetics. It is taken to be equal to the number of ligands added sequentially to Fe^+ before the occurrence of a sharp drop in the rate of ligation. A drop is considered to be sharp if the measured rate coefficient for ligation changes by 2 or more orders of magnitude. Such a drop was observed for all of the ligands investigated. This is clearly evident from Figure 14, which shows that the coordination number observed with the alkanes, alkenes, and alkynes investigated in this study depends on the nature of the hydrocarbon and occasionally on its size. Thus, the coordination number for all alkanes was observed to be 2, for alkenes to be 3 (or 2 for the larger alkenes 1,3-butadiene and isobutene), and for the alkynes to be 3 (but perhaps only 2 for diacetylene). Also "higher order" coordination was observed with the alkynes leading to "secondary" coordination number of at least 5. A common feature of the early ligation kinetics is an increase in the rate coefficient of ligation from the first to the second addition. This increase is particularly large (over 1 order of magnitude) for the small ligands ethane, ethylene, and acetylene. The decrease in the rate coefficient for the first two reactions with butane includes the influence of the occurrence of bimolecular product channels in the first reaction with butane.

F. Structures and Bonding in Ligated Fe^+. *Fe(alkane)$_n^+$.* There has been considerable discussion in the literature of the possible structures and bonding of Fe^+ ligated with a single alkane (HR) molecule including "cluster ions" Fe^+(alkane), the C−H bond insertion adduct H−Fe^+−R, the C−C bond insertion adduct CH_3-Fe^+-R', rearranged species of the type $Fe^+(H_2)$-(alkene) and bridged structures of the type $Fe^+\cdot\cdot H\cdot\cdot R$.[9b] The

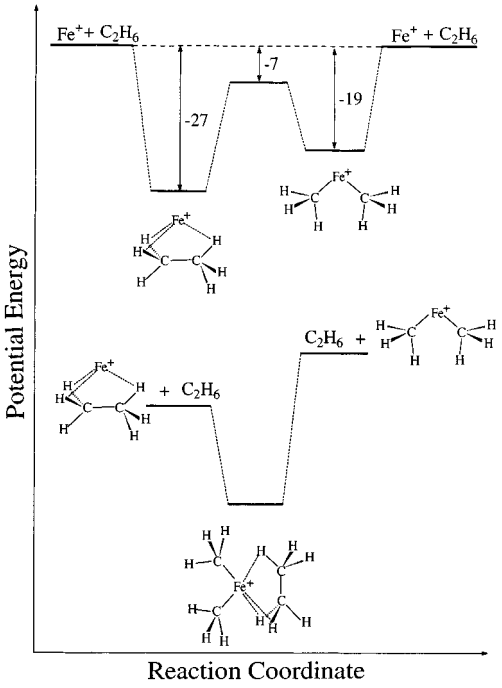

Figure 15. Possible structures and profiles of potential energy vs reaction coordinate for the single and double ligation of Fe^+ with ethane. Structures and energies (in kcal mol^{-1}) for single ligation are taken from ref 3c.

bonding has been treated qualitatively in terms of long-range electrostatic and shorter-range "donor−acceptor" and chemical attractive forces as well as long-range electron−electron repulsion. The bonding in Fe^+ multiply ligated with alkanes also has been addressed, but only very briefly.[9b] The order in bond dissociation energy $BDE(Fe^+-CH_4) < BDE((CH_4)Fe^+-CH_4) \cong BDE((CH_4)_2Fe^+-CH_4) > BDE((CH_4)_3Fe^+-CH_4)$ has been rationalized in terms of spin changes in the core Fe^+ configuration.[2a] The first comprehensive quantum-chemical investigation (a DFT/HF hybrid approach) of an $FeC_nH_{2n+2}^+$ cation has appeared only very recently for the interaction of Fe^+ with ethane.[3b,c] The results of these investigation indicate bound states in the potential energy surface involving "electrostatic" bonding, C−C bond insertion and C−H bond insertion. All three states and the connecting transition states lie below the initial energy of Fe^+ and ethane. Since the PE minimum for $H-Fe^+-C_2H_5$ is extremely shallow (1 kcal mol^{-1}) and only 9 kcal mol^{-1} below the energy of the separated reactants, we can suggest that the singly-ligated $FeC_2H_6^+$ species formed under our operating conditions is likely to be bound as either the "electrostatic" adduct or the C−C insertion adduct as indicated in Figure 15 or as a mixture of the two. It follows that a second molecule of ethane may then bond in an analogous fashion to form the combined electrostatic/inserted species $(C_2H_6)Fe(CH_3)_2^+$ with a structure also shown in Figure 15. Clearly, coordination with six hydrogen atoms to form an electrostatically-bound "sandwich", $Fe^+(C_2H_6)_2$, is not feasible. Also, the doubly-inserted species, $Fe(CH_3)_4^+$, is unlikely because there are not enough unpaired electrons to form four covalent bonds. The further addition of a third molecule of ethane to the electronically saturated doubly-ligated $(C_2H_6)Fe(CH_3)_2^+$ is unlikely for electronic and probably also steric reasons, and this would explain the sharp drop observed for the rate of ligation after the addition of two molecules of ethane. Our CID measurements suggest that the second molecule of ethane is weakly bound when comparing the threshold for its dissociation with the dissociation thresholds of other ligated ions.[17]

Quantum-chemical investigations have not been reported for propane or butane, but the Fe^+/ethane system may well be representative of Fe^+/alkane systems generally. Schematic potential energy curves have been proposed for the ligation of Fe^+ with a single propane molecule but largely with a view to rationalizing H_2 and CH_4 elimination channels via C−H activation and insertion.[4b,c,10] One of these models proposes a barrier to formation of the C−C insertion adduct which lies above the energy of the separated reactants, but this suggestion has not been confirmed by quantum-chemical calculations.[4c]

Fe(alkene)$_n^+$. The bonding of alkenes to the Fe^+ ion has two components: π donation to a σ-like sp^n hybrid orbital and a back-donation from filled d orbitals into the *antibonding* orbital on the C═C double bond. For adducts of the type $FeC_2R_4^+$, including the adducts of Fe^+ with ethylene, propene, and isobutene, such bonding leads to a configuration in which the R substituents are expected to be out of the [Fe,C═C] plane. The bonding of Fe^+ to allene should be similar. The ligation to each double bond should be independent since the adjacent double bonds have π electrons located in two perpendicular planes which cannot be donated to the same center. In contrast, Fe^+ can ligate concomitantly to both double bonds in 1,3-butadiene in either a cis or a trans configuration. Quantum-chemical calculations for these singly-ligated species are generally not available although calculations have been reported for $FeC_2H_4^+$.[5b,c] The lowest-energy state for this ion has been predicted to be a $^4B_2$ state with $D_e = 25.7$ kcal mol^{-1} at the MCPF level of theory[5b] while an optimized geometry is available at QCISD(T) level of theory.[5b]

No quantum-chemical calculations or qualitative potential energy curves are available for higher levels of ligations with any of these hydrocarbons. However, the degree of ligation may be rationalized in terms of consecutive π-electron-pair donation which is determined by the number of available empty orbitals and so the multiplicity of Fe^+. For example, the Fe^+-(^{6}D) ground-state sp^3 configuration has only three places available for two-electron donor ligation (the fourth is occupied by one unpaired electron) while the ^{4}F state allows four two-electron donors to be ligated. The results in Figure 14, which indicate high rates of addition up to three alkene ligands, are consistent with three two-electron-donor ligation to the Fe^+-(^{6}D) ground state or three two-electron-donor ligation to the Fe^+(^{4}F) state in which the addition of the fourth ligand is sterically hindered. Some support for the latter mode of ligation comes from the observation of the slow addition of a fourth molecule of ethylene and the already relatively slow addition of the third molecule of isobutene. Another possible mode of bonding involves oxidative addition which leads to conventional covalent bonds. Six covalent bonds (two per ligand) are possible since Fe^+ has seven available electrons. The remaining one electron cannot form an additional two bonds with a fourth ligand. Ligation of Fe^+ with 1,3-butadiene is a special case because, as described in the next section, it involves intramolecular interligand interactions.

Fe(alkyne)$_n^+$. The bonding of Fe^+ to alkynes is expected to be similar to that with alkenes: π donation to a σ-like sp^n hybrid orbital of Fe^+ and back-donation from filled d orbitals into an antibonding orbital on the C≡C unit. The additional donation of the perpendicular electron pair would turn alkynes formally into four-electron-donor ligands, but we have nothing to support this mode of ligation. The observed fast addition of the first three ligands is similar to the behavior with alkenes.

A theoretical treatment of the bonding of Fe^+ to acetylene indicates electrostatic bonding and a ligand geometry very similar to that of free acetylene.[6] No quantum-chemical

TABLE 2: Collision-Induced Dissociations Observed for Selected Ligated Fe^+ Ions in Which Intramolecular Interactions between Ligands Has Been Proposed To Occur

reaction	threshold energy[a]
$Fe(1,3\text{-}C_4H_6)_4^+ + He \rightarrow Fe(1,3\text{-}C_4H_6)_2^+ + [(1,3\text{-}C_4H_6)_2] + He$	0.220 ± 0.003
$Fe(C_2H_2)_3^+ + He \rightarrow Fe^+ + [(C_2H_2)_3] + He$	1.64 ± 0.13
$Fe(C_2H_2)_5^+ + He \rightarrow Fe(C_2H_2)_3^+ + [(C_2H_2)_2] + He$	0.740 ± 0.060
$Fe(CH_3C_2H)_2^+ + He \rightarrow Fe^+ + [(CH_3C_2H)_2] + He$	1.27 ± 0.11
$Fe(CH_3C_2H)_4^+ + He \rightarrow Fe(CH_3C_2H)_2^+ + [(CH_3C_2H)_2] + He$	0.573 ± 0.049
$Fe(C_4H_2)_2^+ + He \rightarrow Fe^+ + [(C_4H_2)_2] + He$	1.58 ± 0.10
$Fe(C_4H_2)_4^+ + He \rightarrow Fe(C_4H_2)_2^+ + [(C_4H_2)_2] + He$	0.442 ± 0.032

[a] Dissociation threshold in eV (in the center-of-mass energy frame) measured in helium at 0.35 Torr. The quoted uncertainty is equal to the standard deviation in the threshold energy at the junction of the best fit to the initial ion signal and the best fit to the slope of the fastest decaying portion of the disappearance of the parent ion.

calculations or qualitative potential energy curves have been reported for other alkynes or higher levels of ligations with alkynes. The results in Figure 14 indicate high rates of addition up to three alkyne ligands, which is consistent with three two-electron-donor ligation to the $Fe^+(^6D)$ ground state. However, the addition of diacetylene appears to be an exception since a significant drop in rate is observed already after the addition of two molecules. Furthermore, the addition of up to six ligands was observed with all three of the alkynes investigated in this study, which suggests higher-order ligation modes absent with the alkenes. Indeed, the CID measurements suggest the occurrence of intramolecular interligand interactions mediated by Fe^+ for all three alkynes.

G. Intramolecular Interligand Interactions. Now we consider possible intramolecular interactions *between ligands* mediated by Fe^+. Evidence for such interactions comes from the results of the CID experiments. Although in most instances dissociation of the ligated species was observed to proceed one ligand at a time, this was not the case with $Fe(1,3\text{-}C_4H_6)_4^+$ (see Figure 8), $Fe(C_2H_2)_3^+$ and $Fe(C_2H_2)_5^+$ (see Figure 10), $Fe(CH_3C_2H)_2^+$ and $Fe(CH_3C_2H)_4^+$ (see Figure 11), and $Fe(C_4H_2)_2^+$ and $Fe(C_4H_2)_4^+$(see Figure 12) for which observed dissociations led to the loss of the equivalent of two or three molecules. The observed dissociations thresholds for these ions are summarized in Table 2. We propose that in each of these multiply-ligated ions a chemical interaction, mediated by Fe^+, occurs intramolecularly between two or more ligands.

Thus, we attribute the observed exclusive loss of $[(C_2H_2)_3]$ from $Fe(C_2H_2)_3^+$ to the intramolecular isomerization of this ion to $Fe(C_6H_6)^+$ with loss of C_6H_6. Evidence for this particular isomerization was sought in separate CID experiments with $Fe(C_6H_6)^+$ produced directly from the addition of benzene to Fe^+ according to reaction 12. Figure 16 compares the CID spectra

$$Fe^+ + C_6H_6 + He \rightarrow Fe(C_6H_6)^+ + He \qquad (12)$$

of the $Fe(C_2H_2)_3^+$ and $Fe(C_6H_6)^+$ ions produced in these two different ways under otherwise similar operating conditions, and clearly there is a match in the dissociation thresholds measured for these two ions. The actual values obtained for the dissociation threshold (in the center-of-mass energy frame)[17] are 1.64 ± 0.13 and 1.70 ± 0.10 eV, respectively. The similarity in these two values provides strong evidence for the occurrence of the isomerization of $Fe(C_2H_2)_3^+$ to $Fe(C_6H_6)^+$. The failure of the $Fe(C_2H_2)_3^+$ ion produced in reaction 12 to dissociate back to the reactants $Fe(C_2H_2)_2^+ + C_2H_2$ under CID conditions indicates that any barrier to isomerization lies below the initial energy of the reactants and that the isomerization is energetically feasible. The $Fe(C_6H_6)^+$ isomer must be considerably more stable than the $Fe(C_2H_2)_3^+$ isomer given the high exothermicity for the trimerization of acetylene to benzene (-143 kcal mol^{-1}),[19] although not enough thermochemical

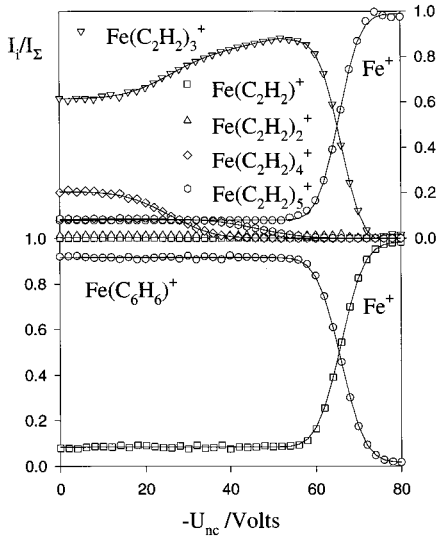

Figure 16. Multicollisional CID results for $Fe(C_2H_2)_3^+$ and $Fe(C_6H_6)^+$ in helium at 0.35 Torr. $Fe(C_2H_2)_3^+$ was formed upstream of the CID region from the sequential ligation of Fe^+ with acetylene (at a flow of 6×10^{18} molecule s^{-1} of acetylene) while $Fe(C_6H_6)^+$ was produced from the ligation of Fe^+ with a single molecule of benzene (at a flow of 1×10^{17} molecule s^{-1} of benzene vapor).

information is available to be completely quantitative. Aside from the match in the CID spectra, the substantial magnitude of the threshold observed for the dissociation (1.64 ± 0.13 and 1.70 ± 0.10 eV) is consistent with the substantial binding energy of 49.6 ± 2.3 kcal mol^{-1} determined experimentally for $Fe^+-C_6H_6$.[20] Our failure to observe the direct formation of $Fe^+ + C_6H_6$ according to reaction 13, which is also expected to be

$$Fe(C_2H_2)_2^+ + C_2H_2 \rightarrow Fe^+ + C_6H_6 \qquad (13)$$

considerably exothermic, suggests that the bulk of the excess energy associated with the isomerization appears in the C_6H_6 ligand rather than the $Fe^+-C_6H_6$ bond. Consequently, we conclude that the third addition of acetylene to Fe^+ occurs in the three steps (14a) to (14c). Apparently, the lifetime for isomerization is shorter than the time required for stabilizing collisions with helium.

$$Fe(C_2H_2)_2^+ + C_2H_2 \rightarrow (Fe(C_2H_2)_3^+)^* \qquad (14a)$$

$$(Fe(C_2H_2)_3^+)^* \rightarrow (Fe(C_6H_6)^+)^* \qquad (14b)$$

$$(Fe(C_6H_6)^+)^* + He \rightarrow Fe(C_6H_6)^+ + He \qquad (14c)$$

Other experimental evidence for the isomerization of $Fe(C_2H_2)_3^+$ to $Fe(C_6H_6)^+$ has been reported previously for $Fe(C_2H_2)_3^+$ produced in a chemical ionization source from sequential bimolecular displacement reactions of type 2.[12] High-

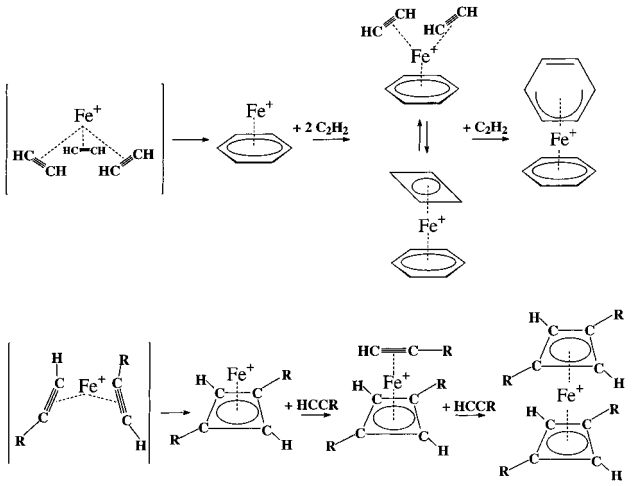

Figure 17. Proposed mechanisms for the multiple ligation of Fe^+ with actylene, propyne (R = CH_3) and diacetylene (R = C_2H) involving intramolecular interligand interactions.

energy collision-induced dissociation experiments indicated that at least a fraction of these ions had isomerized to $Fe(C_6H_6)^+$. More recently, FT-ICR/CID experiments have shown in a related study that at least a fraction of the $Fe_4(C_2H_2)_3^+$ ions produced by the sequential dehydrogenative addition of ethylene according to reaction 15 isomerizes to $Fe_4(C_6H_6)^+$ prior to collisional dissociation.[21]

$$Fe_4(C_2H_2)_n^+ + C_2H_4 \rightarrow Fe_4(C_2H_2)_{n+1}^+ + H_2 \qquad (15)$$

Other higher-order intramolecular interligand chemistry with acetylene is revealed by the results of the CID experiments reported here. We attribute the observed loss of the equivalent of two molecules of acetylene from $Fe(C_2H_2)_5^+$ compared to the loss of one molecule of acetylene from $Fe(C_2H_2)_4^+$ (see Figure 10) to the formation of a cyclobutadienyl ring (a rich electron donor) in $Fe(C_2H_2)_5^+$ as shown in Figure 17. The CID spectrum indicates that $Fe(C_2H_2)_5^+$ is more strongly bound than $Fe(C_2H_2)_4^+$: the dissociation thresholds for the loss of $(C_2H_2)_2$ from $Fe(C_2H_2)_5^+$ and loss of C_2H_2 from $Fe(C_2H_2)_4^+$ are 0.740 $\pm$ 060 and 0.329 $\pm$ 0.025 eV, respectively. The intensity of the $Fe(C_2H_2)_6^+$ ion formed by ligating $Fe(C_2H_2)_5^+$ with one additional molecule of acetylene was too small for a CID study. The "T-shaped" structure for $Fe(C_2H_2)_6^+$ proposed in Figure 17 involves sideways 4π electron bonding to a second benzene ring to be consistent with the 18-electron rule.

The observed dissociations of the higher-order Fe^+ ions ligated with propyne and diacetylene are markedly different from that observed with acetylene: the third adduct loses one ligand molecule while the *second* adduct loses *two* according to the generalized reactions 16 and 17. We propose in this case that

$$Fe(L)_3^+ + He \rightarrow Fe(L)_2^+ + L \qquad (16)$$

$$Fe(L)_2^+ + He \rightarrow Fe^+ + [(L)_2] \qquad (17)$$

Fe^+ mediates the cyclization of the first two ligands into dimethyl- and diethynylcyclobutadiene, respectively, as shown in Figure 17. The antiaromatic cyclobutadiene ring is intrinsically unstable, but in these ligated ions we propose that it is stabilized by bonding to Fe^+ and by the presence of two methyl or ethynyl substituents. We note in comparison that Fe^+ does not seem to mediate the isomerization of two molecules of acetylene to cyclobutadiene since the CID of $Fe(C_2H_2)_2^+$ indicated exclusive loss of *one* molecule of acetylene. Apparently, the additional electron donor properties of two methyl groups and two electron-rich ethynyl groups are required to stabilize a four-membered ring in the multiple ligation of Fe^+ by propyne and diacetylene, respectively.

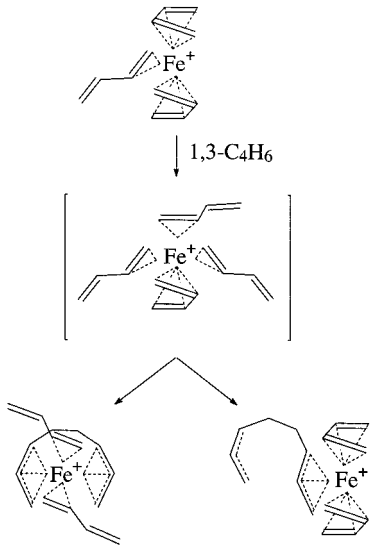

Figure 18. Proposed mechanism for the multiple ligation of Fe^+ with 1,3-butadiene involving intramolecular interligand interactions.

The addition of two further molecules of propyne to Fe(propyne)$_2^+$ and of diacetylene to Fe(diacetylene)$_2^+$ resulted in ligated species which again dissociated with the loss of the equivalent of two molecules of propyne or diacetylene, respectively, according to reaction 18. Again we propose the occurrence of intramolecular cyclization as shown in Figure 17.

$$Fe(L)_4^+ + He \rightarrow Fe(L)_2^+ + [(L)_2] \qquad (18)$$

Finally, we note that the collision-induced dissociation of the fourth adduct of Fe^+ with 1,3-butadiene, Fe(1,3-butadiene)$_4^+$, was observed to result in the loss of the equivalent of two molecules of 1,3-butadiene. We interpret this observation in terms of a dimerization of 1,3-butadiene after the addition of the fourth molecule in a η^6 coupling reaction as illustrated in Figure 18. Such a reaction may lead to an "open" $Fe^+(\eta^4\text{-}cis\text{-}1,3\text{-}C_4H_6)_2(\eta^3\text{-}C_8H_{12})$ structure (which has several cis/trans isomers) and a "closed" $Fe^+(\eta^2\text{-}trans\text{-}1,3\text{-}C_4H_6)_2(\eta^6\text{-}C_8H_{12})$ structure in which the dimer is coordinated as a three- and a six-dentate ligand, respectively.

Conclusions

The experimental results reported here provide a broad survey of the intrinsic kinetics for ligation of Fe^+ with saturated and unsaturated acyclic hydrocarbons at room temperature in helium at 0.35 Torr. Trends in the rates of addition of one ligand with the size of the ligand are consistent with expectations in terms of the degrees of freedom and stability of the ligated species according to current models of ion/molecule association reactions. The observed variations of the measured rate coefficients for the sequential ligation of Fe^+ provide insight into the intrinsic coordination number of Fe^+ for acyclic hydrocarbons. Intramolecular interligand interactions mediated by Fe^+ were found to be relatively common among the larger unsaturated hydrocarbon ligands. This unexpected result has been attributed to intramolecular oligomerization and cyclization reactions.

Acknowledgment. D.K.B. is grateful to the Natural Sciences and Engineering Research Council of Canada for the financial support of this research and to S. Wlodek and H. Wincel for

their useful contributions in the first stages of this project. H.B. thanks Professor H. Schwarz and the Fonds der Chemischen Industrie for financial supprt.

References and Notes

(1) (a) Eller, K.; Schwarz, H. *Chem. Rev.* **1991**, *91*, 1121. (b) Armentrout, P. B. In *Selective Hydrocarbon Activation: Principles and Progress*, Davies, J. A., Watson, P. L., Liebman, J. F., Greenberg, A., Eds.; VCH: New York, 1990; pp 467−533. (c) Weisshaar, J. C. *Acc. Chem. Res.* **1993**, *26*, 213.

(2) (a) Schultz, R. H.; Armentrout, P. B. *J. Phys. Chem.* **1993**, *97*, 596. (b) Perry, J. K.; Ohanessian, G.; Goddard, W. A. *J. Chem. Phys.* **1993**, *97*, 5238. (c) Perry, J. K., Ph.D. Dissertation, California Institute of Technology, 1993. (d) Bauschlicher, C. W.; Sodupe, M. *Chem. Phys. Lett.* **1993**, *214*, 489. (e) Ricca, A.; Bauschlicher, C. W.; Rosi, M. *J. Phys. Chem.* **1994**, *98*, 9498.

(3) (a) Schultz, R. H.; Armentrout, P. B. *J. Phys. Chem.* **1992**, *96*, 1662. (b) Holthausen, M. C.; Fiedler, A.; Schwarz, H.; Koch, W. *Angew. Chem., Int. Ed. Engl.* **1995**, *34*, 2282. (c) Holthausen, M. C.; Fiedler, A.; Schwarz, H.; Koch, W. *J. Phys. Chem.* **1996**, *100*, 6236.

(4) (a) Schultz, R. H.; Armentrout, P. B. *J. Am. Chem. Soc.* **1991**, *113*, 729. (b) Hanton, S. D.; Noll, R. J.; Weisshaar, J. C. *J. Phys. Chem.* **1992**, *96*, 5176. (c) Van Koppen, P. A. M.; Bowers, M. T.; Fisher, E. R.; Armentrout, P. B. *J. Am. Chem. Soc.* **1994**, *116*, 3780.

(5) (a) Jacobson, D. B.; Freiser, B. S. *J. Am. Chem. Soc.* **1983**, *105*, 7484. (b) Sodupe, M.; Bauschlicher, C. W.; Langhoff, S. R.; Partridge, H. *J. Phys. Chem.* **1992**, *96*, 2118, 5760. (c) Schröder, D.; Fiedler, A.; Schwarz, H. *Int. J. Mass Spectrom. Ion Processes* **1994**, *134*, 239.

(6) Sodupe, M.; Bauschlicher, C. W. *J. Phys. Chem.* **1991**, *95*, 8640.

(7) (a) Van Koppen, P. A. M.; Jacobson, D. B.; Illies, A.; Bowers, M. T.; Hanratty, M.; Beauchamp, J. L. *J. Am. Chem. Soc.* **1989**, *111*,1991. (b) Schultz, R. H.;Armentrout, P. B.*Organometallics* **1992**, *11*, 828.

(8) Peake, D. A.; Gross, M. L. *Organometallics* **1986**, *5*, 1236.

(9) (a) Tonkyn, R.; Weisshaar, J. C. *J. Phys. Chem.* **1986**, *90*, 2305. (b) Tonkyn, R.; Roman, M.; Weisshaar, J. C. *J. Phys. Chem.* **1988**, *92*, 92.

(10) Van Koppen, P. A. M.; Kemper, P. R.; Bowers, M. T. *J. Am. Chem. Soc.* **1992**, *114*, 10941.

(11) Jacobson, D. B.; Freiser, B. S. *J. Am. Chem. Soc.* **1983**, *105*, 5197.

(12) Schröder, D.; Sülzle, D.; Hrusak, J.; Bohme, D. K.; Schwarz, H. *Int. J. Mass Spectrom. Ion Processes* **1991**, *110*, 145.

(13) Mackay, G. I.; Vlachos, G. D.; Bohme, D. K.; Schiff, H. I. *Int. J. Mass Spectrom. Ion Phys.* **1980**, *36*, 259.

(14) Raksit, A. B.; Bohme, D. K. *Int. J. Mass Spectrom. Ion Processes* **1983**, *55*, 69.

(15) Baranov, V.; Javahery, G.; Hopkinson, A. C.; Bohme, D. K. *J. Am. Chem. Soc.* **1995**, *117*, 12801.

(16) Brandsma, L. *Preparative Acetylenic Chemistry*; Elsevier: New York, 1971.

(17) Baranov, V.; Bohme, D. K. *Int. J. Mass Spectrom. Ion Processes* **1996**, *154*, 71.

(18) Armentrout, P. B.; Kickel, B. L. In *Organometallic Ion Chemistry*, Freiser, B. S., Ed.; Kluwer Academic Publishers: Dordrecht, 1996; pp 1−45.

(19) Lias, S. G.; Bartmess, J. E.; Liebman, J. F.; Holmes, J. L.; Levin, R. D.; Mallard, W. G. *J. Phys. Chem. Ref. Data* **1988**, *17* (Suppl. 1), 1.

(20) Meyer, F.; Khan, F. A.; Armentrout, P. B. *J. Am. Chem. Soc.* **1995**, *117*, 9740.

(21) Gehret, O.; Irion, M. P. *Chem. Phys. Lett.* **1996**, *254*, 379.